



# Biochar from oil cakes: an efficient and economical adsorbent for the removal of acid dyes from wool dye house effluent

Seiko Jose<sup>1</sup> · Reena Roy<sup>2</sup> · Ava Rani Phukan<sup>2</sup> · Dinesh Babu Shakyawar<sup>1</sup> · Anuradha Sankaran<sup>3</sup>

Received: 8 August 2021 / Accepted: 4 December 2021 / Published online: 17 January 2022  
© The Author(s), under exclusive licence to Springer-Verlag GmbH Germany, part of Springer Nature 2021

## Abstract

In the reported study, biochars were prepared from almond, coconut, and mustard oil cakes by chemical activation with phosphoric acid followed by low-temperature pyrolysis. The ball milling technique was employed to reduce the particle size of the biochars below 300 nm. The synthesized biochars were characterized by various analytical techniques like Fourier Transform Infrared Spectroscopy, Scanning Electron Microscopy, X-ray diffraction spectroscopy, BET surface analysis, porosity measurement, methylene blue value and further employed for the removal of color from the acid dye effluent from the wool dyeing unit. The results showed that very small quantities (2.0 %) of biochars are sufficient to remove around 92% color from the dye effluent. The adsorption properties of the synthesized biochars were found to be greatly depending on the type of oil cake used. Among the three selected oil cakes, *viz.* mustard, coconut, and almond, the later was found to be performed well in terms of color removal. The batch adsorption and kinetic studies indicate the second order pathway of color removal for the synthesized biochars.

---

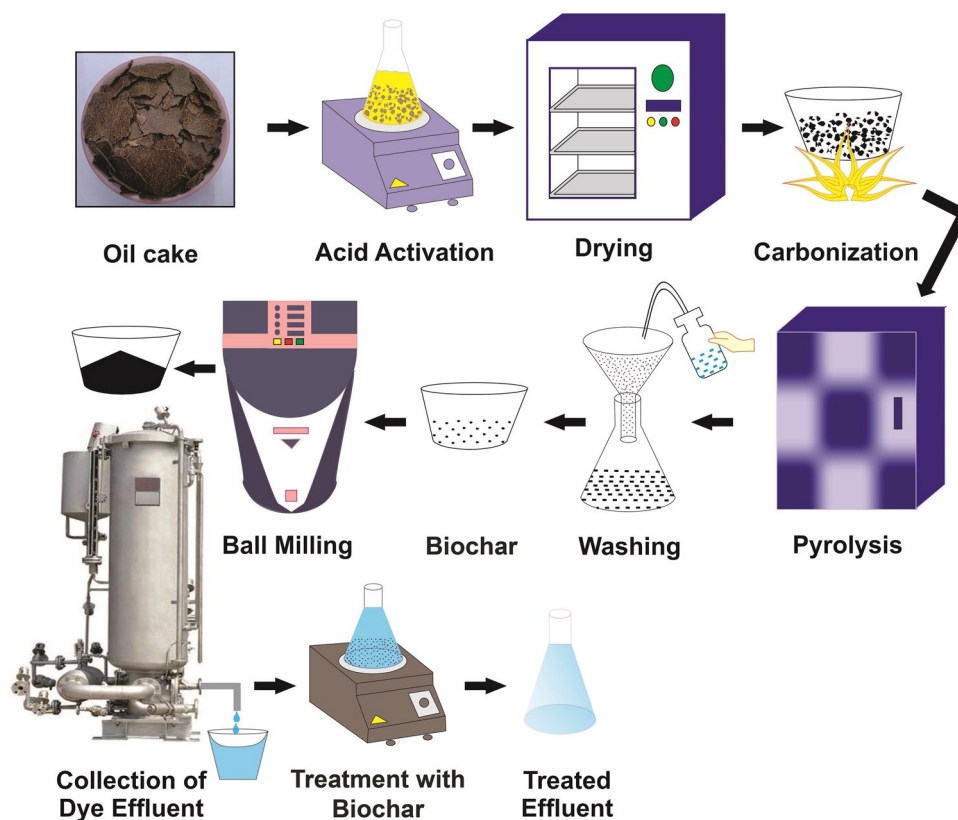
✉ Seiko Jose  
seiko\_jose2005@yahoo.co.in

<sup>1</sup> Textile Manufacturing and Textile Chemistry Division,  
ICAR - Central Sheep and Wool Research Institute,  
Avikanagar, Malpura 304501, India

<sup>2</sup> Department of Textiles and Apparel Design, Assam  
Agricultural University, Jorhat, Assam 785013, India

<sup>3</sup> Department of Chemistry, PSNA College of Engineering  
and Technology, Dindigul, Tamil Nadu 624622, India

## Graphical Abstract



**Keywords** Acid dyes · Biochar · Dye removal · Effluent treatment · Oil cakes

## Introduction

During the dyeing of textiles, depending upon the class of dye and the nature of the textile fiber, it is estimated that 15–20 % of the dyes remained in the dye bath and discharged as effluent. The dye house effluents may contain heavy metals, ammonia, acids, alkalies, salts, and large amounts of pigments, many of which are toxic and low bio-degradable materials (Crini 2006; Mohan and Karthikeyan 2004). The textile industrial effluents are subjected to various treatments before discharging into the water bodies or land. The main methods used to treat colored effluents are oxidation, activated carbon, coagulation, flocculation, biological treatment, advanced oxidation process (AOP), and membrane filtration. The disposal of improperly treated dye house effluent may cause a menace to the quality of the receiving water bodies, the aquatic eco-system, and humans due to objectionable color, odor, high biological oxygen demand (BOD) and chemical oxygen demand (COD), total dissolved solids (TDS), and other toxic compounds (Jose et al. 2020). In particular, acid dyes are widely employed in wool and silk dyeing industries. Such textile dyes are typically very stable

with half-lives of 2–13 years in the environment, and they have been detected in several rivers, lakes, and terrestrial soils, causing toxicological problems to the aquatic environment (Copaciu et al. 2016).

Oil cakes as an agro-residue are obtained after the extraction of oil from dried kernels. Early days, oil cakes had not acquired much commercial value except as feed for cattle and poultry. However, new technologies open up enormous potential for oil cakes and it is reported to have the potentiality in the production of enzymes, antioxidants, antibiotics, vitamins, biopesticides, etc (Ramachandran et al. 2007). Pyrolysis is the conventional method of preparation of activated carbon and biochar. During this process, the ligno cellulosic biomass is converted into solid carbon particles by the release of volatile matter. The yield and properties of the activated carbon and biochar greatly depend on the raw materials, activating chemicals, and pyrolysis conditions (Yuan et al. 2020; Jandačka et al. 2017). The high cost of activated carbon restricts its use as a commercial adsorbent. Biochars prepared from agro-residues such as rice husk, rice straw, hazelnut shell, pine needles, wheat straw, and sunflower straw could find potential applications in pesticide

and heavy metal removal (Dawood et al. 2017), fertilizers, porous carbon catalysts (Wang and Wang 2019; Panahi et al. 2020; Vaughn et al. 2018), etc. In particular, phosphoric acid (H<sub>3</sub>PO<sub>4</sub>) treatment of biochar has been reported to improve the surface area, micropore structures, carbon retention without increasing energy and sorption capacity (Zhao et al. 2017; Chu et al. 2018). The carbon rich biochar was already explored as soil enhancer and the phosphoric acid treated biochar finds its application as an eco-friendly P-rich fertilizer.

Today activated carbon derived from petroleum products is commonly employed for the color removal of textile dye effluent. The main objective of the study is the exploration of oil cakes, which is a bio-waste, for the color removal from the industrial dye effluent. As of today, a dearth of literature is available on the preparation of biochar from oil cakes and its further use in the removal of real dye house effluent. Further, most of the reports are focused on study of adsorption properties of biochar synthesized from a single oil cake and a comparative study with a number of biochars synthesized from various oil cakes are not reported. In the present attempt, biochars were prepared from almond, coconut, and mustard oil cakes through chemical activation followed by pyrolysis. The physical and adsorption characteristics of the biochars were investigated. The synthesized biochars were employed for the removal of color from acid dyes of real textile dye effluent from the wool processing pilot plant using batch adsorption experimental studies.

### Materials and methods

Oil cakes used for the study were collected directly from oil mills from various locations of India and used without further purification. Optilan Turquoise (acid dye) was purchased from local dye suppliers, Jaipur, India. Chemicals, viz. orthophosphoric acid (assay–98 %) and acetic acid (assay–99.5 %), were purchased from Merck, India.

### Collection of dye effluent

The effluent used for the study was taken from the wool dyeing pilot plant at M/S Central Sheep and Wool

Research Institute, Avikanagar, Rajasthan, India. The dyeing of wool fabric with acid dye (10 g/l Optilan Turquoise) was performed by maintaining 1:20 material to liquid ratio (MLR) keeping the pH 5.0 using acetic acid. This particular pH is maintained in the dye bath since it is the operational pH of acid dyes in the aqueous medium. The dyeing was carried out at 90 °C for 30 min without using any auxiliaries, except 0.5 g/L nonionic wetting agent (Ultravon, JU). After dyeing, the effluent was collected, filtered, and used for the characterization and batch experimental studies.

### Preparation of biochars

The oil cakes of almond, coconut, and mustard were pulverized in a grinder. The finely powdered oil cakes were filtered through 200 mesh size nylon filter to get particles of almost the same size. Three hundred grams of each powder were individually triggered to acid activation using 1.0 N and 2.5 N orthophosphoric acid for 24 h, with continuous stirring in a mechanical shaker. The impregnation ratio of acid to oil cakes was kept at 4:1. After acidification, the oil cakes were squeezed to remove the acid and dried at 105 °C for 60 min. The dried oil cakes were then charred and further pyrolyzed in a muffle furnace at 350 °C for 2 h with a heating rate of 20°C/min in air atmosphere. The biochar thus obtained was washed with hot and then cold water to attain neutral pH and dried. The yield of biochar was calculated using Eq. (1),

$$\text{Yield of Biochar} = (\text{Weight of biochar/weight of oil cake}) \times 100 \tag{1}$$

The particle size of the biochars was further reduced by 2 h of ball milling in Pulverisette (model-6 ClassicLine, Fritsch, Russia). To narrow down the experiment, a preliminary exercise was conducted. The dye effluent was treated with a 0.5 % weight percentage of each adsorbent for 30 min and the absorbency values were noted (Table 1). Based on the absorbency value, the best one from each oil cake was selected for further characterization and batch adsorption studies, namely 2.5 N PAB, 1.0 N PCB, and 2.5 N PMB.

**Table 1** Absorbency values of biochar prepared from oil cakes

S. No	Biochars	Abbreviation	Absorbance
1	1.0 N H <sub>3</sub> PO <sub>4</sub> treated almond oil cake biochar	1.0 N PAB	1.20
2	2.5 N H <sub>3</sub> PO <sub>4</sub> treated almond oil cake biochar	2.5 N PAB	1.15
3	1.0 N H <sub>3</sub> PO <sub>4</sub> treated coconut oil cake biochar	1.0 N PCB	1.27
4	2.5 N H <sub>3</sub> PO <sub>4</sub> treated coconut oil cake biochar	2.5 N PCB	1.32
5	1.0 N H <sub>3</sub> PO <sub>4</sub> treated mustard oil cake biochar	1.0 N PMB	1.22
6	2.5 N H <sub>3</sub> PO <sub>4</sub> treated mustard oil cake biochar	2.5 N PMB	1.10

## Characterization of biochars

The particle size of biochar was analyzed using the Malvern Mastersizer (model – 3000) particle size analyzer. FTIR analysis was performed for the identification of functional groups present in the bare oil cakes and the synthesized biochar using the Bruker double beam spectrophotometer (Model—Alpha). The spectra were measured from 4000–500  $\text{cm}^{-1}$ . Dispersion (0.1 %) of biochar in water was sonicated before feeding to the particle size analyzer to deter agglomeration. The morphology of the biochar was analyzed by SEM analysis using Nova Nano FESEM-450 (Netherlands) with suitable magnification. X-ray diffraction analysis was conducted using a Panalytical X'pert powder diffractometer. The surface area analysis of the powdered biochars was performed using Nova Touc LX2 b Quantachrome instrument under nitrogen atmosphere to obtain the adsorption isotherm and the surface area was calculated by Brunauer–Emmett–Teller (BET) method.

## Analysis of physical and adsorption properties of biochars

About 0.1 g of the biochars was added to 30 ml distilled water and boiled for 10 minutes. The solution was brought to room temperature and filtered. The pH of the solution was measured with a pH meter (Hanna- HI98130). For the analysis of bulk density, 3.0 g of adsorbent was taken in a 10 ml measuring cylinder and tightly packed without voids. The density was determined from the ratio of mass to volume. Adsorbent (0.5 g) was kept at 105 °C for 6 h. The moisture content of the adsorbent was analyzed from the difference in the weights before and after drying. For porosity measurement, 2.5 ml distilled water was added to 1.5 g adsorbent in a 10 ml measuring cylinder. The volume of the cylinder was recorded ( $V_1$ ) initially and after one hour ( $V_2$ ) (Pongener et al. 2015). The methylene blue value was determined by dissolving 1.2 g methylene dye in a 1000 ml standard measuring flask with the aid of 0.25 % (v/v) acetic acid. The absorbance of the solution was then adjusted to 0.84 at 620 nm by dilution. Added 0.1 g of the biochar sample with 25 ml of the methylene blue test solution in a volumetric flask and shaken until decolorization has occurred. The addition of methylene blue in the step of 5 ml was continued till the saturation point, *i.e.*, the color persists. The amount of methylene blue added was noted (Nunes and Guerreiro 2011).

## Batch adsorption experiments

The Optilan Turquoise acid dye effluent was treated with the selected biochars in a mechanical shaker with 200 rpm. The color removal efficiencies were recorded in terms of absorbance value. The experiments were conducted at 27 °C

keeping the actual pH (6.9) of the acid dye effluent. The weight percentage of the adsorbents (0.5, 1.0, 1.5, and 2.0 %) and the duration of treatment (30, 60, and 90 min) were kept as variables. After each experiment, the solution was centrifuged, filtered and the absorbency was measured using UV–visible spectrophotometer (Make- Systronics). The reactions were repeated thrice for its reproducibility.

## Kinetic studies

Upon performing the batch adsorption studies, it was observed that 2.5 N PAB is giving the maximum color removal. Thus, the kinetic study of 2.5 N PAB was carried out at different adsorbent dosages. The pseudo-first-order rate Eq. (2) was used to calculate the adsorption capacity of the synthesized biochar given by equation,

$$\ln(q_e - q_t) = \ln q_e - k_1 t \quad (2)$$

where  $q_e$  is the amount of dye adsorbed on adsorbent at equilibrium (mg/g),  $q_t$  is the amount of dye adsorbed at any time (mg/g), and  $k_1$  ( $\text{min}^{-1}$ ) is the rate constant of the pseudo-first-order adsorption which can be calculated from the slope of the linear plot of  $\ln(q_e - q_t)$  against time. The pseudo-second-order expression used to describe the rate of adsorption is presented by equation (3),

$$\frac{t}{q_t} = \frac{1}{k_2 q_e^2} + \frac{1}{q_e^2} t \quad (3)$$

where  $k_2$  ( $\text{g/mg/min}$ ) is the rate constant of the pseudo-second-order adsorption.  $k_2$  and  $q_e$  can be calculated from the slope and intercept of the plot of  $t/q_t$  vs time.

## Results and discussion

### Properties of biochars

The physical properties of the selected biochars are shown in Table 2. The yield of the biochar was found to be a maximum for 2.5 N PMB (9.6 %), followed by 1.0 N PCB (9.4 %), and 2.5 N PAB (8.1 %). During the charring process, the oil cakes undergo shrinkage and the weight loss may due to the loss of moisture content followed by decomposition of cellulosic material and removal of inorganic impurities as ash (Ding et al. 2014). The bulk density of the prepared 2.5 N PAB (0.652  $\text{g/cm}^3$ ) was found to be slightly higher than the others. The value of the bulk density of the prepared biochars is between 0.50 and 0.75  $\text{g/cm}^3$ , which indicates that the prepared biochars are suitable for decolorization applications (Downie et al. 2012). Further, in the later adsorption studies, it is observed that the biochar (2.5 N PAB) with a highest bulk density (0.652  $\text{g/cm}^3$ ) was found to have the

**Table 2** Physical and adsorption properties of biochars

Biochar	Yield (%)	Bulk density (g/cm <sup>3</sup> )	Moisture content (%)	pH	Methylene blue value (mg/g)	Porosity (%)	Mean particle size (nm)
2.5 N PAB	8.1	0.652	21.34	6.6	130	0.346	310 (100)*
1.0 N PCB	9.4	0.625	12.13	6.7	105	0.323	113 (100)*
2.5 N PMB	9.6	0.625	14.21	6.5	120	0.369	140 (92)*

\*Figures in the parenthesis indicates the percentage of intensity of particle

highest color removal efficiency and methylene blue value. The pH values of all synthesized biochars were found to be near neutral because of thorough washing with distilled water.

The dye adsorption capacity of biochars can be well expressed in terms of methylene blue value. Among the three biochars, the highest methylene dye adsorption capacity (130 mg/g) was registered with 2.5 N PAB. One of the governing factors that determine the adsorption capacity of biochar is its porosity. The pores are formed in the biochar due to the release of volatile organic matters. The highest porosity (0.369 %) was observed with 2.5 N PMB followed by 2.5 N PAB (0.349 %). The least porosity (0.323 %) was observed with biochar prepared from 1.0 N PCB. Ball milling is the common method adopting for the reduction of the size of particles through grinding. Even after the same chemical treatment followed by the same period of ball milling, it is observed that the size of the biochar varies significantly depending on the source. The lowest particle size (113 nm) was observed in the case of 1.0 N PCB and the maximum was observed in the case of 2.5 N PAB (310 nm). From the particle size analysis of various biochars, it is observed that among the three biochars, 2.5 N PAB and 1.0 N PCB showed 100 % distribution intensity and the 2.5 N PMB showed more than 90 %. This indicates that the ball milling process was done perfectly, and as a result, all the particles in single biochars showed almost the same particle size (Partlan et al. 2016). Thus, the physical and adsorption studies reveal that the properties of biochar greatly depend on the type of oil cake and concentration of activating acid.

### FTIR analysis

Since in the batch adsorption studies of acid dyes, the biochar prepared from 2.5 N PAB gave the best performance, the FTIR study is being reported for the same in comparison with its source oil cake (Fig. 1). The chemical activation of biochar might promote the surface functional groups and hence influence the adsorption property. In the case of pristine almond oil cake, the sharp peak at 3736 cm<sup>-1</sup> corresponds to the -OH hydroxyl stretching, probably due to the presence of moisture in the oil cake. The band near 1736 cm<sup>-1</sup> is assigned to stretching

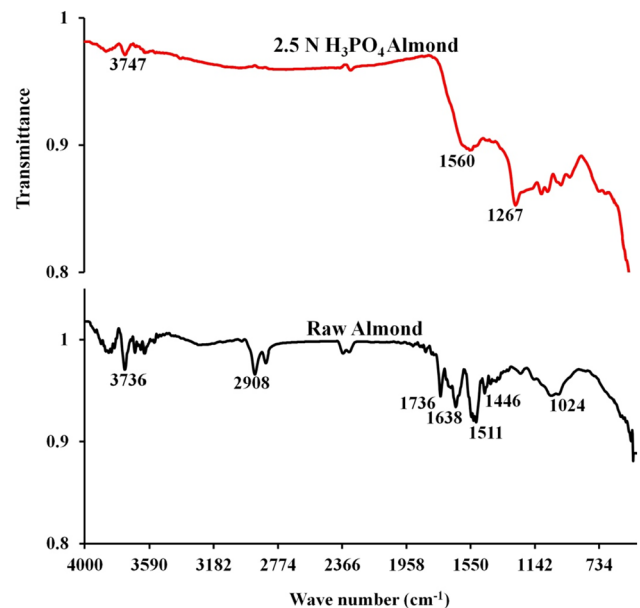


**Fig. 1** FTIR spectra of raw almond oil cake and 2.5 NPAB

vibrations of the C=O of the ester and aldehydic groups present in hemicelluloses and lignin (Basu et al. 2015). The bands around 2908 cm<sup>-1</sup> are attributed to aliphatic C-H asymmetric stretching present mainly in cellulose, which is the major component of the lignocellulosic biomass (Adel et al. 2011). The broad peak at 1024 cm<sup>-1</sup> region ascribed to C=O, C-H, C-O-C, and C-O deformation or stretching vibrations of different groups in cellulose, hemicellulose, and lignin (Pandey et al. 2019). The sharp, but slightly broad peak at 1511 cm<sup>-1</sup> indicates the C=C vibrations of the aromatic rings of lignin (Jose et al. 2017). The C=O stretching vibration in conjugated carbonyl of lignin is shown at 1638 cm<sup>-1</sup> and the aliphatic part of lignin at 1446 cm<sup>-1</sup> (Shi and li 2012). In the case of biochar, after chemical treatment followed by pyrolysis, most of the peaks were disappeared in comparison with pristine oil cake. The peak at 1638 cm<sup>-1</sup> attributes to the removal of oxygen functional groups and the peak at 2908 cm<sup>-1</sup> shows the decomposition of cellulosic structure and the appearance of a new peak at 1267 cm<sup>-1</sup> may be due to the phosphorous-oxygen-carbon stretch (Yakout and



El-Deen 2016). Due to the poor moisture adsorption of the biochar, the peak corresponding to hydroxyl group at  $3747\text{ cm}^{-1}$  is slightly visible.

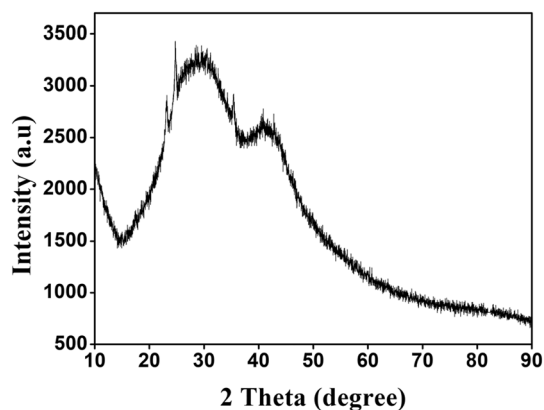


Fig. 2 XRD pattern of 2.5 N PAB

## XRD analysis

The X-ray diffraction pattern of the 2.5 N PAB is displayed in Figure 2. The broad peak reveals the presence of amorphous structure of the biochar with low crystallinity. The peak at  $29^\circ$  perhaps due to the presence of amorphous carbon with the diffraction pattern of (002), which indicates the graphite like structure. Due to the low pyrolysis temperature ( $350^\circ\text{C}$ ), the oil cakes are not fully converted in to carbon, and as a result, the XRD peaks show a small crystalline nature. This is further supported by EDX analysis. The peak at  $43^\circ$  indicates the formation of atomic order with the diffraction of (1 0 0), respectively (Girgis 2007).

## SEM and EDX analysis

The SEM and EDX analysis was performed with the 2.5 N PAB, since it showed best color removal efficiency among the selected biochars (Figures 3, 4).

The surface of the biochar with irregularly shaped pores (2–50 nm) is visible in the SEM images. During the pyrolysis process, the acids react with oil cake and create pores

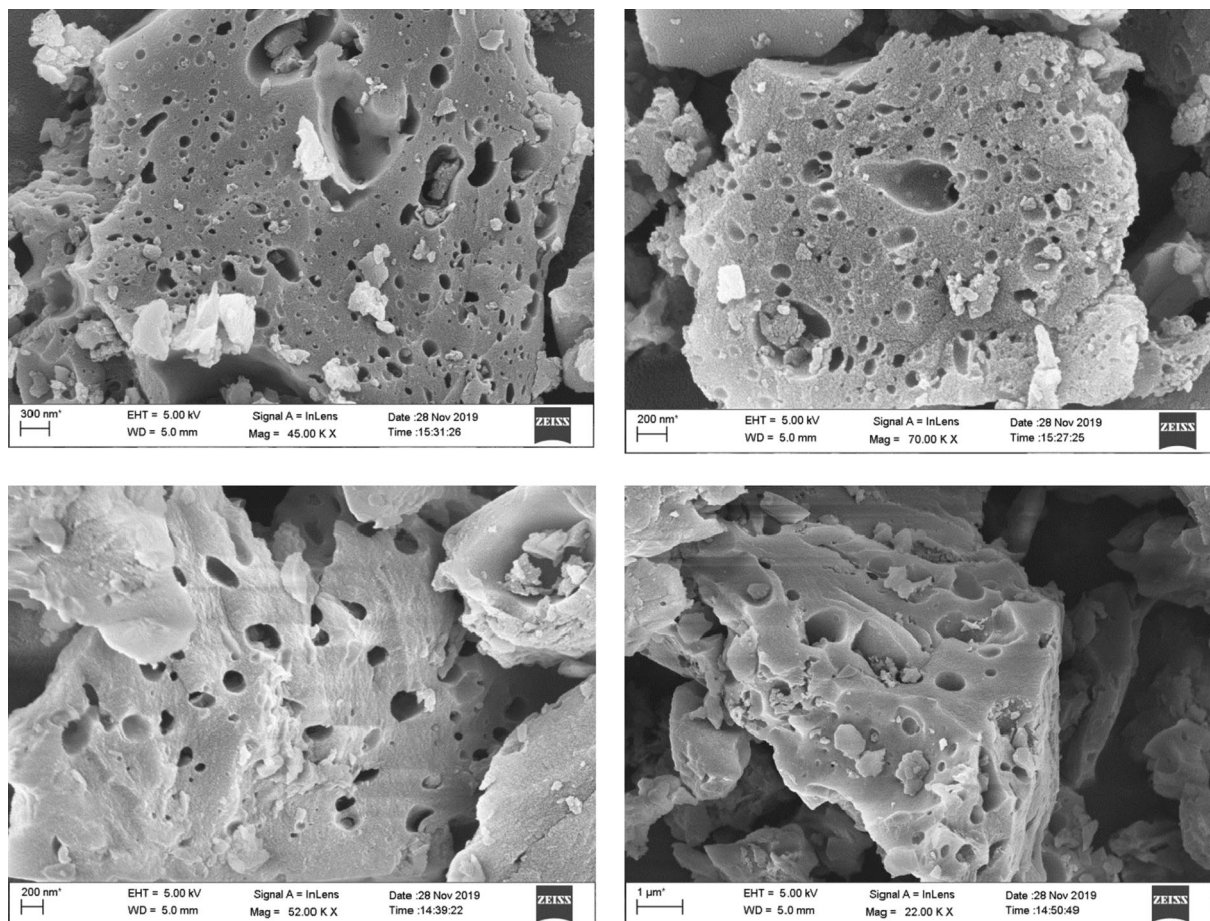


Fig. 3 Scanning electron micrograph images of 2.5 N PAB at various magnifications

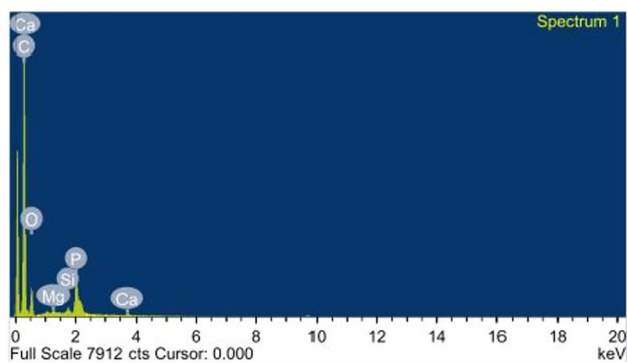


Fig. 4 EDX spectra of 2.5 N PAB

due to the evaporation of volatile gases (Yue 1995). The number of pores per unit area produced by H<sub>3</sub>PO<sub>4</sub> treated almond is high as confirmed by porosity studies. The size and shape of the pores are found to be non-uniform. The highly porous structure of the biochar can account for the higher methylene blue value and color removal efficiencies. The EDX analysis depicted that the 2.5 N PAB is rich in carbon content (83.67). In addition to carbon and oxygen, a negligible quantity of P, Mg, Ca, and Si was also detected.

Table 3 depicts the elemental analysis of 2.5 N PAB biochar. It shows 83.67 % carbon and 14.85% oxygen. The presence of higher concentration of oxygen may be due to low temperature pyrolysis (350°C), which didn't convert the whole oil cake into carbon. Other elements like Si, Mg, P, and Ca are present in negligible quantities.

**BET analysis**

One of the critical parameters of biochar is its BET surface area to characterize the adsorption phenomenon. The surface area of the biochar is a key factor in determining the efficiency of color removal. In general, the surface area, pore volume, and average pore size increased with residence time and pyrolytic temperature (Tushar et al. 2012). The BET analysis of 2.5 N PAB was performed as described earlier, and the results are tabulated in Fig. 5. There is a robust association exists between the carbon content of the biochar and BET surface area. Pyrolysis leads to the degradation of organic material of oil cakes and improves the surface area of 85.78 m<sup>2</sup>/g. There have also been plausible studies of similar findings elsewhere (Thangalazhy-Gopakumar et al. 2015). The surface area of biochar produced from biomass is less than that of activated carbon produced from

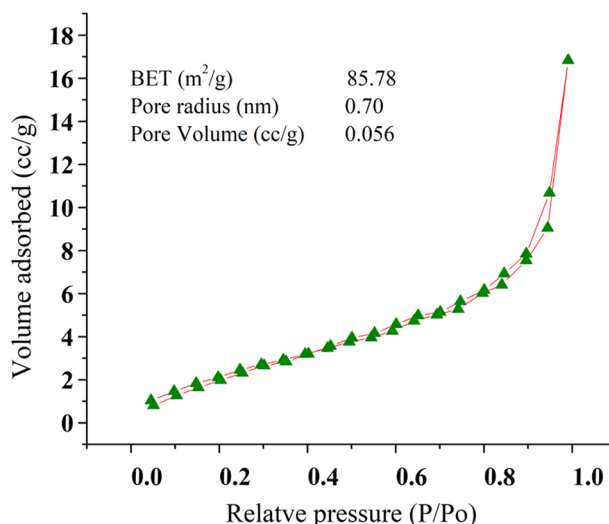


Fig. 5 BET analysis image of 2.5 N PAB

the same sources due to low temperature pyrolysis (Batista et al. 2018). The pore radius and pore volume (0.70 nm and 0.056 cc/g) indicate the presence of herbaceous biochars. The relatively good pore radius and pore volume may have a key role in the adsorption of the acid dyes from the effluent. The specific surface area, pore volume and pore radius of biochar are highly depend on the raw material, activating chemical and pyrolysis temperature due to the variation in the decomposition of organic matters (Tomczyk et al. 2020).

**Batch adsorption studies**

An attempt has been made to investigate the adsorption capacity of biochars derived at low temperature (350 °C) and feasible conditions. The adsorption studies are directly observed with wool dye house effluent by following the absorbance of the acid dye effluent. Immediately after dyeing, the absorbency of the acid dye effluent was found to be 1.27. In all the selected biochars, there observed an increasing trend in the color removal with respect to time and concentration of adsorbent. Poor color removal efficiencies were recorded with all biochars at a low weight percentage of 0.5 and 1.0 % due to saturation of the adsorption at the surface of the adsorbent and no further decolorization occur. Increasing the weight percentage of adsorbent from 1.5 to 2.0 % resulted in better color removal and attains equilibrium near 90 min, while, among three biochars of 1.5 % concentrations, the efficiency was found to be the highest

Table 3 Elemental composition of 2.5 N PAB though EDX analysis

Sample	C (At wt %)	O (At wt %)	Si (At wt %)	Mg (At wt %)	P (At wt %)	Ca (At wt %)
2.5 N PAB	83.67	14.85	0.13	0.11	1.16	0.08

in the case of 2.5 N PAB than the other two biochars as demonstrated in Fig. 6a. The adsorption studies on color removal from acid dye bath using various concentrations of 2.5 N PAB are shown in Fig. 6b. Among the different weight percentages of biochars (0.5, 1.0, 1.5, and 2.0 %) used for the adsorption studies, the 2.0 % biochar found to be more effective in removing the color in all selected oil cakes. The 2.5 N PAB at the weight percentage of 2.0 % resulted the highest color removal with an absorbency value of 0.1.

### Kinetic studies

The experimental and calculated values of  $k_1, k_2, q_e$ , and regression coefficient values ( $R^2$ ) for acid dyes are given in Table 4. Pseudo-first-order kinetic model fit linearly up to 30 to 40 minutes with regression values of 0.99 and deviation occurs beyond this time. This shows that the adsorption process is fast initially, and after that the attainment of saturation of active sites takes place depending upon the amount of adsorbent. The pseudo-second-order kinetics fit well with rate expression with  $R^2$  values showing that the rate of adsorption equilibrium capacity increases with the amount of adsorbent (Fig 7). The results revealed that the saturation of adsorbent attained at a lower adsorbent percentage and the rate of adsorption augment with an increase in

weight percentage of adsorbent. The amount of acid dye adsorbed on 2.5 N PAB is found to be quite high may result from high methylene blue value as in Table 2.

### Conclusion

An attempt was made to prepare biochars from oil cakes and used for the removal of the color of the acid dye from wool dye effluent. Phosphoric acid treatment followed by a low temperature pyrolysis converted the oil cakes into biochars. We concluded the study with the following inferences.

- SEM images confirmed the pore structure in the biochar, which helps in the adsorption of the acid dyes.
- The adsorption process was found to be rapid in the initial stage of adsorption and gradually became stable after attaining the saturation of active sites.
- Among various biochars prepared from different oil cakes, the biochar developed from almond (2.5 N PAB) was found to have better color removal efficiency than others with 92 % color removal.
- The batch adsorption and kinetic studies indicate the second order pathway of color removal with the highest

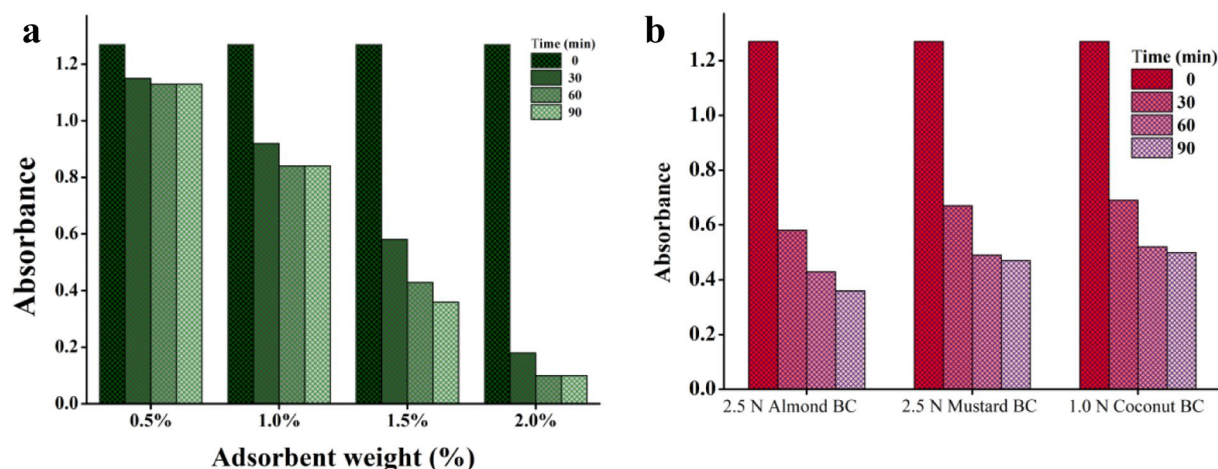


**Fig. 6** a Batch adsorption studies on acid dye removal using 2.5 NPAB, b Batch adsorption studies on acid dye removal using 1.5 weight percentage of phosphoric acid treated biochars

**Table 4** Pseudo-first-order and pseudo-second-order values for acid dye adsorption by 2.5 N PAB

Adsorbent in weight (%)	Experimental $q_e$ ( $\text{mg}\cdot\text{g}^{-1}$ )	Pseudo-first-order			Pseudo-second-order		
		$q_e$ ( $\text{mg}\cdot\text{g}^{-1}$ )	$k_1$ ( $\text{min}^{-1}$ )	$R^2$	$q_e$ ( $\text{mg}\cdot\text{g}^{-1}$ )	$k_2$ ( $\text{g}\cdot\text{mg}^{-1}\cdot\text{min}^{-1}$ )	$R^2$
0.5	8.06	9.87	0.0654	0.99	13.11	0.0025	0.99
1.0	5.03	4.37	0.0700	0.99	05.99	0.0179	0.99
1.5	4.04	3.96	0.1151	0.99	04.28	0.0607	0.99
2.0	3.12	1.16	0.1285	0.99	03.18	0.2999	0.99



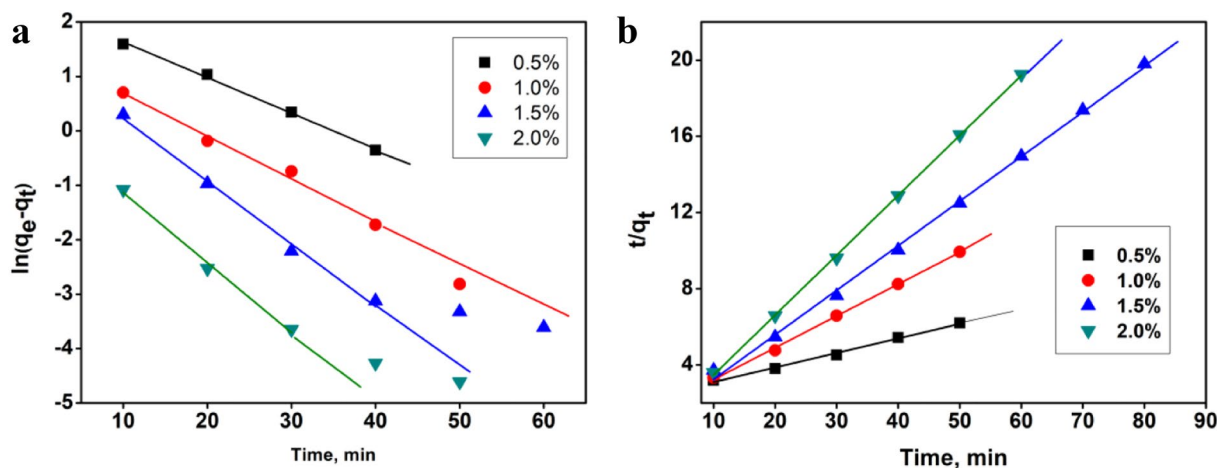


Fig. 7 Kinetic plots of adsorption of acid dye on 2.5 N PAB **a** Pseudo-first-order, **b** Pseudo-second-order

efficiency of the biochar derived from almond oil cake, followed by mustard and coconut.

- This may be due to the high surface area ( $85.78 \text{ m}^2/\text{g}$ ) of the biochar. The XRD studies reveal the high amorphous structure of the biochar.
- Irrespective of the source, in all cases of biochars, the color removal efficiency was found to be directly proportional to the concentration of adsorbents.

Thus, it may be concluded that the biochar derived from oil cakes can effectively be utilized for the removal of color from real acid dye effluent.

## References

- Adel AM, Abd El-Wahab ZH, Ibrahim AA, Al-Shemy MT (2011) Characterization of microcrystalline cellulose prepared from lignocellulosic materials Part II: physicochemical Properties. *Carbohydr Polym* 83(2):676–687
- Basu G, Mishra L, Jose S, Samanta AK (2015) Accelerated retting cum softening of coconut fibre. *Ind Crop Pro* 77:66–73
- Batista EM, Shultz J, Matos TT, Fornari MR, Ferreira TM, Szpoganicz B, de Freitas RA, Mangrich AS (2018) Effect of surface and porosity of biochar on water holding capacity aiming indirectly at preservation of the Amazon biome. *Sci Rep* 8(1):1–9
- Chu G, Zhao J, Huang Y, Zhou D, Liu Y, Wu M, Peng H, Zhao Q, Pan B, Steinberg CEW (2018) Phosphoric acid pretreatment enhances the specific surface areas of biochars by generation of micropores. *Environ Pollut* 240:1–9
- Copaciu F, Opris O, Niinemets Ü, Copolovici L (2016) Toxic influence of key organic soil pollutants on the total flavonoid content in wheat leaves. *Water Air Soil Pollut* 227(6):1–10
- Crini G (2006) Non-conventional low-cost adsorbents for dye removal: a review. *Bioresour Technol* 97(9):1061–1085
- Dawood S, Sen TK, Phan C (2017) Synthesis and characterization of slow pyrolysis pine cone bio-char in the removal of organic and inorganic pollutants from aqueous solution by adsorption: kinetic, equilibrium, mechanism and thermodynamic. *Bioresour Technol* 246:76–81
- Ding W, Dong X, Ime IM, Gao B, Ma LQ (2014) Pyrolytic temperatures impact lead sorption mechanisms by bagasse biochars. *Chemosphere* 105:68–74
- Downie A, Crosky A, Munroe P (2012) Physical properties of biochar. *Biochar for environmental management*. Routledge, Cambridge, pp 45–64
- Girgis BS, Temerk YM, Gadelrab MM, Abdullah ID (2007) X-ray diffraction patterns of activated carbons prepared under various conditions. *Carbon Lett* 8(2):95–100
- Jandačka J, Mičieta J, Holubčík M, Nosek R (2017) Experimental determination of bed temperatures during wood pellet combustion. *Energy Fuels* 31(3):2919–2926
- Jose S, Mishra L, Basu G, Kumar Samanta A (2017) Study on reuse of coconut fiber chemical retting bath. Part II—recovery and characterization of lignin. *J Nat Fibers* 14(4):510–518
- Jose S, Shanmugam N, Kumar A, Das S (2020) Removal of basic violet from wool dyeing effluent using nanoparticles. *J Nat Fibers* 19:1–11
- Mohan SV, Karthikeyan J (2004) Adsorptive removal of reactive azo dye from an aqueous phase onto charfines and activated carbon. *Clean Technol Environ Policy* 6(3):196–200
- Nunes CA, Guerreiro MC (2011) Estimation of surface area and pore volume of activated carbons by methylene blue and iodine numbers. *Quim Nova* 34:472–476
- Panahi HK, Dehghani M, Ok YS, Nizami AS, Khoshnevisan B, Musatto SI, Aghbashlo M, Tabatabaei M, Lam SS (2020) A comprehensive review of engineered biochar: production, characteristics, and environmental applications. *J Clean Prod* 270:122462
- Pandey R, Patel S, Pandit P, Nachimuthu S, Jose S (2018) Colouration of textiles using roasted peanut skin—an agro processing residue. *J Clean Prod* 172:1319–1326
- Partlan E, Davis K, Ren Y, Apul OG, Mefford OT, Karanfil T, Lader DA (2016) Effect of bead milling on chemical and physical characteristics of activated carbons pulverized to superfine sizes. *Water Res* 89:161–170
- Pongener CH, Kibami DA, Rao KS, Goswamee RL, Sinha D (2015) Synthesis and characterization of activated carbon from the bio-waste of the plant *Manihot esculenta*. *Chem Sci Trans* 4(1):59–68

- Ramachandran S, Singh SK, Larroche C, Soccol CR, Pandey A (2007) Oil cakes and their biotechnological applications—a review. *Biore-sour Technol* 98(10):2000–2009
- Shi J, Li J (2012) Metabolites and chemical group changes in the wood-forming tissue of *Pinus koraiensis* under inclined conditions. *Bio Resources* 7(3):3463–3475
- Tomczyk A, Sokołowska Z, Boguta P (2020) Biochar physicochemical properties: pyrolysis temperature and feedstock kind effects. *Rev Env Sci Biotechnol* 19(1):191–215
- Tushar MSHK, Mahinpey N, Khan A, Ibrahim H, Kumar P, Idem R (2012) Production, characterization and reactivity studies of chars produced by the isothermal pyrolysis of flax straw. *Biomass Bio-energ* 37:97–105
- Vaughn SF, Dinelli FD, Jackson MA, Vaughan MM, Peterson SC (2018) Biochar-organic amendment mixtures added to simulated golf greens under reduced chemical fertilization increase creeping bentgrass growth. *Ind Crop pro* 111:667–672
- Wang J, Wang S (2019) Preparation, modification and environmental application of biochar: a review. *J Clean Prod* 227:1002–1022
- Yakout SM, El-Deen GS (2016) Characterization of activated carbon prepared by phosphoric acid activation of olive stones. *Arab J Chem* 9:S1155–S1162
- Yuan T, He W, Yin G, Xu S (2020) Comparison of bio-chars formation derived from fast and slow pyrolysis of walnut shell. *Fuel* 261:116450
- Yue ZR (1995) Preparation of activated carbon fibers and adsorption mechanism of Ag<sup>+</sup>. Ph.D. dissertation. Zhongshan University, Guangzhou.
- Zhao L, Zheng W, Masek O, Chen X, Gu B, Sharma BK, Cao X (2017) Roles of phosphoric acid in biochar formation: Synchronously improving carbon retention and sorption capacity. *J Environ Qual* 46(2):393–401

**Publisher's Note** Springer Nature remains neutral with regard to jurisdictional claims in published maps and institutional affiliations.